diversity

MDPI

Article

Microbial Community Abundance Affects the Methane Ebullition Flux in Dahejia Reservoir of the Yellow River in the Warm Season

Yi Wu [1,2], Xufeng Mao [1,2,*], Liang Xia [1,2], Hongyan Yu [3], Yao Yu [3], Wenjia Tang [4], Feng Xiao [5] and Haichuan Ji [5]

[1] MOE Key Laboratory of Tibetan Plateau Land Surface Processes and Ecological Conservation, Qinghai Normal University, Xining 810008, China
[2] School of Geographical Science, Academy of Plateau Science and Sustainability, Qinghai Normal University, Xining 810008, China
[3] Management and Service Center of Qilian Mountain National Wetland Park, Xining 810008, China
[4] State Key Laboratory for Environmental Protection Monitoring and Assessment of the Qinghai-Xining Plateau, Xining 810007, China
[5] Qinghai Forestry and Grass Bureau, Xining 810007, China
* Correspondence: maoxufeng@yeah.net; Tel.: +86-139-0978-7689

Abstract: Reservoirs are an integral part of the global carbon cycle and generally considered to be methane (CH_4) emission hot spots. Although remarkable research achievements have been made concerning CH_4 ebullition from inland waters, such as rivers, lakes, and ponds, few have been devoted to CH_4 ebullition from plateau reservoirs. The present study focused on CH_4 ebullition from the Dahejia Reservoir located in the upper reaches of the Yellow River. We analyzed the spatial and temporal characteristics of CH_4 ebullition flux across the water-atmosphere interface between July and August 2021. We also evaluated the influence of microbes on CH_4 ebullition flux. The results showed that (1) CH_4 ebullition was the dominant mode of CH_4 emissions in the study site, which contributed to 78.85 ± 20% of total CH_4 flux. (2) The mean CH_4 ebullition flux in the nighttime (0.34 ± 0.21 mg m^{-2} h^{-1}) was significantly higher than that in the daytime (0.19 ± 0.21 mg m^{-2} h^{-1}). The mean CH_4 ebullition flux first decreased and then increased from the upstream (0.52 ± 0.57 mg m^{-2} h^{-1}) to the downstream (0.43 ± 0.3 mg m^{-2} h^{-1}) of the Yellow River. (3) Sediment microbes affected the CH_4 ebullition flux primarily by changing the microbial community abundance. The regression analysis showed that CH_4 ebullition flux had a significantly linear negative correlation with microbial abundance in sediments. The redundancy analysis further showed CH_4 ebullition flux was significantly positively correlated with the abundances of Firmicutes and Actinobacteria, and negatively with that of Proteobacteria and Chloroflexi. Among abiotic variables, CH_4 ebullition flux was closely related to total phosphorus, total organic carbon, pH and nitrate nitrogen.

Keywords: CH_4; ebullition flux; plateau reservoir; microbes

Citation: Wu, Y.; Mao, X.; Xia, L.; Yu, H.; Yu, Y.; Tang, W.; Xiao, F.; Ji, H. Microbial Community Abundance Affects the Methane Ebullition Flux in Dahejia Reservoir of the Yellow River in the Warm Season. *Diversity* **2023**, *15*, 154. https://doi.org/10.3390/d15020154

Academic Editors: Peng Hou, Weiguo Jiang, Wei Li and Li Zhang

Received: 24 October 2022
Revised: 24 December 2022
Accepted: 18 January 2023
Published: 21 January 2023

1. Introduction

Global warming has been deteriorating since the age of industrial revolution. From 1750 to 2021, the atmospheric methane (CH_4) concentration increased from 722 ppb to 1889 ppb, by 162% [1]. CH_4 is one of the three primary greenhouse gases. On the centennial scale, the warming potential of CH_4 is maximally 28 times that of carbon dioxide [2]. In the past century, CH_4 has accounted for roughly 20% of the global temperature increase. CH_4 is not only an important food and energy source in the freshwater food web, but also occupies an irreplaceable place in the carbon cycle of aquatic ecosystems [3]. The increase in atmospheric CH_4 concentration has undergone three stages on the temporal scale. The first stage is the growth stage (8.4 ± 0.6 ppb $year^{-1}$) and the second is the stable stage (0.4 ± 0.5 ppb $year^{-1}$). The third stage, which is believed to have started in 2007, is

another rapid growth stage (7.9 ± 0.6 ppb year^{-1}) [4]. The increasing atmospheric CH_4 concentration has caused a series of environmental safety problems, such as aggravating climate change, glacier melt, and permafrost thaw. However, the natural or human factors that are dominant in the above processes, remains unknown and attracts growing academic interest.

Currently, most estimates of CH_4 balance are usually carried out by replacing the total CH_4 emissions with CH_4 diffusion, while ignoring CH_4 ebullition [5]. The global freshwater ecosystem emitted 93.1 Tg CH_4 into the atmosphere every year, with CH_4 ebullition accounting for about 59% (55.3 Tg CH_4) [6]. Under extreme conditions, CH_4 ebullition may be several dozen times that of emissions by diffusion [7]. The most intensively studied influence factors of CH_4 emission fluxes from inland water bodies include meteorological factors (wind speed, atmospheric pressure), water quality factor (pH, dissolved oxygen, nutrient salts), hydrological factors (water depth, water velocity, water temperature), and ecosystem productivity [8–10]. In addition to environmental factors, CH_4 ebullition flux is also influenced by microbes. The global aquatic ecosystem emitted 576 Tg CH_4 every year, most of which was produced by methanogens, but more than half of which was oxidized to carbon dioxide by methanotrophs. In marine ecosystems, more than 90% of CH_4 was consumed by methanotrophs [11–13]. Therefore, mitigation of CH_4 emissions from aquatic ecosystem requires more attention to the relevant microbes [14].

The Qinghai-Tibet Plateau has been substantially influenced by global climate change, and the influence pattern is considered more complex than in many other places in the world. Global climate change has brought significant changes to the ecosystem composition, including hydrology, soil, climate, and biology [15,16]. Although the Qinghai-Tibet Plateau shows a lower temperature than that of many tropical zones, there are abundant psychrotolerant methanogens, indicating sustained metabolic activity even during the cold season [17]. In addition, low atmospheric pressure due to the high altitude facilitates significantly CH_4 ebullition emissions from the lakes and rivers of the Qinghai-Tibet Plateau [18,19]. Unlike natural aquatic ecosystems such as lakes and rivers, the water level of plateau reservoirs fluctuates more greatly and frequently due to human control [20]. The corresponding changes in hydrostatic pressure and alteration of redox conditions in the reservoir ecosystem have prompted CH_4 production and emissions [21]. These things considered, reservoir fluids are in a static state and associated with longer hydraulic retention time and lower dissolved oxygen concentration in water bodies and sediments compared with natural aquatic ecosystem [22]. Therefore, the CH_4 supersaturation and ebullition are common occurrences in reservoirs. A growing body of evidence has shown that water bodies in the Qinghai-Tibet Plateau are CH_4 emissions hotspots [19,23]. A more accurate estimate of global CH_4 emissions is hardly possible without the basic data from the Qinghai-Tibet Plateau. In the present study, we first analyzed the spatial and temporal characteristics of CH_4 ebullition flux across the water—atmosphere interface between July and August 2021. We then evaluated the influence of biotic and abiotic factors on CH_4 ebullition flux, in the hope of laying the foundation for in-depth investigation of CH_4 ebullition flux in plateau reservoirs.

2. Study Sites

The Dahejia Reservoir (102°45′8.80″ E, 35°50′10.44″ N) of the Yellow River is located in the hinterland area inhabited by Chinese ethnic minorities (Figure 1). Sitting along the trunk stream of the Yellow River at the junction between Guanting Town of Huzhu Tu Autonomous County in the Qinghai Province and Dahejia Town of Jishishan Bonan, Dongxiang and Salar Autonomous County, the Dahejia Reservoir is the twelfth cascade hydropower station under the hydropower development plan for the Longyang Gorge-Qingtong Gorge subregion of the Yellow River. The geomorphology around the reservoir is featured by the alternation between gorges and plains. The terrain is flat with conspicuous gullies on the two banks. The reservoir is 75 to 120 m wide during the flat water period. The water depth is mainly controlled by the upstream hydropower station and fluctuates

widely, ranging from 1.8 to 5.6 m. The study site has a continental climate. Located deep in the northwest inland and far from the sea, the Dahejia Reservoir has large diel and annual temperature ranges, with little rainfall throughout the year and large evaporation. Due to high frequency of harsh weather events in winter, including Siberian high and cold waves, the average minimum temperature over the years is as low as −11.6 °C. The precipitation in this region increases as temperature increases in spring. The local precipitation further increases in summer and autumn as the Pacific subtropical high extends towards the west. Precipitation in these two seasons makes a greater contribution to annual precipitation compared with spring and winter, accounting for about 70%. The subregion surrounding the reservoir is dominated by cultivated plants, which are occasionally interspersed with natural vegetation, including coniferous forests, brush, grassland, and meadow. Light gray calcareous soil is the predominant soil type in the study site. Despite the high land use diversity, the land utilization level remains low [24].

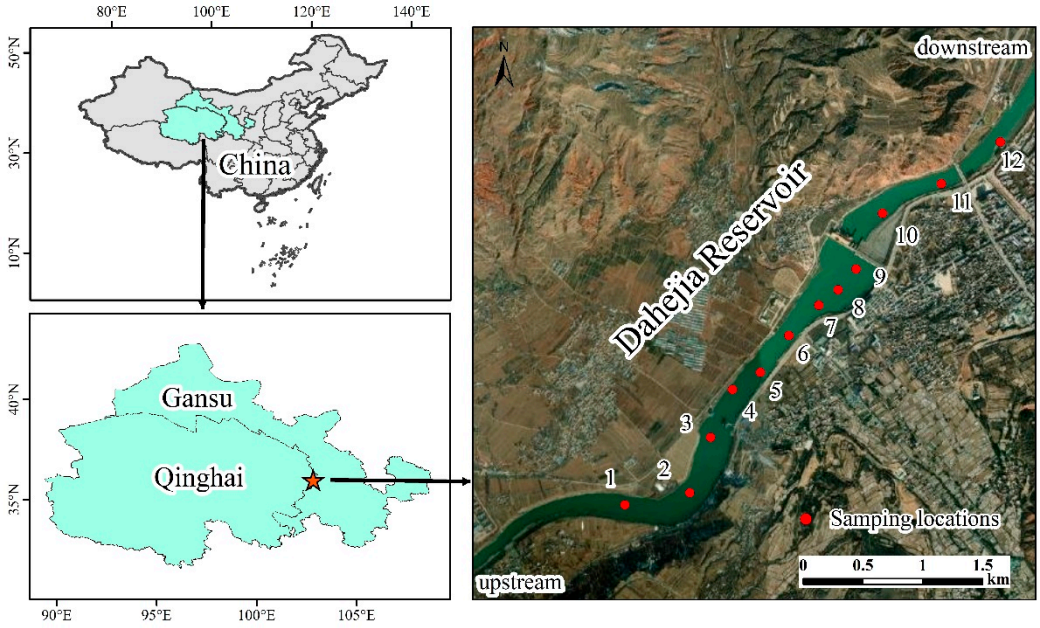

Figure 1. Location map of the study site. Twelve sampling points were subdivided into four subregions: River (1–3), Middle (4–6), Lake (7–9), and Down (10–12).

3. Materials and Methods

3.1. CH_4 Fluxes Monitoring

The study site extended from 2 km upstream to 1 km downstream of the Dahejia Reservoir. From upstream to downstream of the reservoir, the study site was subdivided into four subregions: River, Middle, Lake, and Down, as shown in Figure 1. In each subregion three sampling points were set up, and there were 12 sampling points in total. From July 29 to 31, 2021, CH_4 fluxes across the water-atmosphere interface were monitored on the diel scale for River, Lake, and Down subregions at a time interval of six hours. From August 1 to 18, 2021, 12 sampling points were monitored during the daytime. CH_4 fluxes across the water-atmosphere interface were measured using the static chamber-gas chromatography-based method [17]. Using the headspace equilibrium technique [25], the concentration of CH_4 in water samples was measured on a gas chromatography (Agilent 7890B, Santa Clara, CA, USA) equipped with a flame ionization detector.

Total CH_4 flux (F_t, μmol m^{-2} d^{-1}) was monitored using a static chamber and calculated according to the equation below [17]:

$$F_t = \frac{n_t - n_0}{At} \quad (1)$$

n_t and n_0 are CH_4 gas concentrations in the static chamber at time t and the initial moment 0 (mol), respectively. A is the surface area of the static chamber above water (m^2). t is the monitoring duration (min).

The CH_4 diffusion flux (F_d, μmol m^{-2} d^{-1}) is calculated using the thin-boundary layer method [26]:

$$F_d = k \times \left(C_{water} - C_{equilibrium}\right) \quad (2)$$

k is the gas diffusion rate (cm h^{-1}); $C_{water}$is the dissolved CH_4 concentration in the water body (μmol L^{-1}); $C_{equilibrium}$is the equilibrium concentration of CH_4 in the water body under actual conditions (μmol L^{-1}). CH_4 saturation in the surface water (%) is C_{water}divided by $C_{equilibrium}$. CH_4 ebullition flux (F_e, μmol m^{-2} d^{-1}) is defined as the total CH_4 flux minus the diffusion flux.

3.2. High-Throughput Sequencing

High-throughput sequencing was conducted by Beijing Biomarker Technologies using the Illumina NovaSeq 6000 system [27]. After microbial total DNA extraction from the sediments with a FastDNA SPIN Kit for Soil (MP Biomedicals, Santa Ana, CA, USA), we carried out real-time PCR, followed by product purification, quantification, and homogenization. A sequencing library was built and subjected to a quality check. If the library was eligible, it was then sequenced using the Illumina NovaSeq 6000 sequencing platform (Illumina, San Diego, CA, USA). The sequencing data analysis consisted of the following steps: (1) raw read processing: the raw reads were subjected to preliminary screening, with the low-quality reads filtered out and leaving only the high-quality ones. (2) operational taxonomic unit (OTU) clustering and species annotation: Usearch was employed for OTU clustering at 97% identity threshold, and the number of OTU was determined [28]. Thus, the high-quality reads were denoised and clustered into OTU. Then, based on the sequence compositions of OTU, we obtained the species abundance for different taxonomic ranks (phylum, class, order, family, genus, and species).

3.3. Collection and Measurement of Environmental Data

A Van Veen grab sampler with a mouth measuring 1/40 m^2 was used to collect sediments at a depth of 0–15 cm at the specified sampling sites. The sediments were passed through a 2 mm sieve, placed into a 20 mL centrifuge tube, and transported back to the laboratory in a car refrigerator at 4 °C (PHILIPS TB5301, Amsterdam, The Netherlands). The colorimetric method was used to measure the total phosphorus, total nitrogen, nitrate nitrogen concentrations with Autoanalyser-3 (Seal Analytical, Norderstedt, Germany). The total dissolved carbon of the sediment was measured by a total organic analyzer (Shimadzu Corp, Kyoto, Japan). In the meantime, environmental parameters were acquired at about 0.5 m below the water surface at each sampling site using HQ40d portable water quality monitor (Hach, Loveland, CO, USA), including dissolved oxygen, water temperature, pH, salinity, and total dissolved solid. Water samples were collected using a 2 L stainless steel water sampler into a 1 L water sample bottle. They were used to determine the water quality indicators. The water depth and velocity were directly measured with doppler velocity meter (BOYIDA LSH10-1QC, Xiamen, China). The wind speed, air temperature, and air pressure were measured at 1 m above the water surface using a portable anemometer (Testo 480, Lenzkirch, Germany).

3.4. Statistical Analyses

Correlation analysis and one-way analysis of variance (ANOVA) were carried out using SPSS 24.0. A p-value smaller than 0.05 was statistically significant. Three duplicate samples were collected to determine the above parameters and indicators, and the results were expressed as mean ± standard deviation. R-3.6.3 was run to carry out redundancy analysis (RDA) of the correlation between the primary microbes and environmental variables, and statistical graph plotting.

4. Results

4.1. The CH_4 Ebullition Flux Was Higher in the Nighttime than in the Daytime

Table 1 shows the dissolved CH_4 concentration, saturation, and contribution of CH_4 ebullition flux in the surface water of the Dahejia Reservoir in the daytime and the nighttime. The diel variation range of CH_4 concentration in the surface water of the Dahejia Reservoir was 0.11–0.43 μmol L^{-1}. In the daytime, the CH_4 concentration fell within the range of 0.26–0.43 μmol L^{-1}; in the nighttime, it varied within the range of 0.11–0.37 μmol L^{-1}. An independent-samples T-test showed no significant differences in the mean CH_4 concentration in the daytime (0.34 ± 0.06 μmol L^{-1}) and the nighttime (0.28 ± 0.08 μmol L^{-1}) ($p > 0.05$). Both in daytime and nighttime, the dissolved CH_4 concentration was significantly higher than the equilibrium concentration in the water body. The CH_4 saturation in the surface water of the Dahejia Reservoir varied within the range of 81–6885%. In the daytime, the CH_4 saturation fell within the range of 157–6885%; in the nighttime, it fell within the range of 81–5189%. An independent-samples T-test showed that the mean CH_4 saturation in the daytime (1732 ± 2803%) and the nighttime (1433 ± 2378%) was not significantly different ($p > 0.05$). The contribution of CH_4 ebullition flux in the daytime to total CH_4 flux at the reservoir varied within the range of 16.47–92.92%; In the nighttime, it varied within the range of 80.35–100%. An independent-samples T-test showed that the mean contribution of CH_4 ebullition flux in the nighttime (95.65 ± 7.97%) was significantly higher than that in the daytime (68.01 ± 26.23%) ($p < 0.05$).

Table 1. Dissolved CH_4 concentration, saturation, and contribution of CH_4 ebullition flux in the Dahejia Reservoir at different time.

Time	CH_4 Concentration (μmol L^{-1})	CH_4 Saturation (%)	Contribution of CH_4 Ebullition Flux (%)
Daytime (06:00–18:00)	0.34 ± 0.06 ^{a}	1732 ± 2803 ^{a}	68.01 ± 26.23 ^{a}
Nighttime (18:00–06:00)	0.28 ± 0.08 ^{a}	1433 ± 2378 ^{a}	95.65 ± 7.97 ^{b}

^{a,b} Values having different subscript letters in the same column are significantly different from each other ($p < 0.05$).

Figure 2 shows the temporal characteristics of CH_4 diffusion and ebullition flux across the water—atmosphere interface of the Dahejia Reservoir in the daytime and the nighttime. According to our measurements, the diel variation range of CH_4 diffusion flux across the water—atmosphere interface was 0–0.14 mg m^{-2} h^{-1}. In the daytime, the CH_4 diffusion flux fell within the range of 0.01–0.14 mg m^{-2} h^{-1}; in the nighttime, it varied within the range of 0–0.1 mg m^{-2} h^{-1}. An independent-samples T-test showed no significant differences in the mean CH_4 diffusion flux in the daytime (0.06 ± 0.05 mg m^{-2} h^{-1}) and the nighttime (0.02 ± 0.04 mg m^{-2} h^{-1}) ($p > 0.05$). The diel variation range of CH_4 ebullition flux across the water—atmosphere interface was 0.03–0.69 mg m^{-2} h^{-1}. In the daytime, the CH_4 ebullition flux fell within the range of 0.03–0.69 mg m^{-2} h^{-1}; in the nighttime, it varied within the range of 0.07–0.6 mg m^{-2} h^{-1}. An independent-samples T-test showed that the mean CH_4 ebullition flux in the nighttime (0.34 ± 0.21 mg m^{-2} h^{-1}) was significantly higher than that in the daytime (0.19 ± 0.21 mg m^{-2} h^{-1}) ($p < 0.05$).

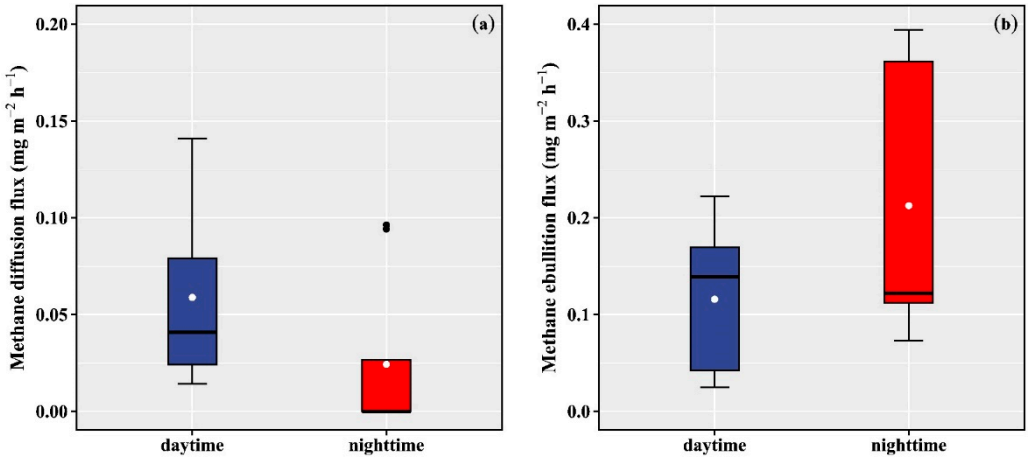

Figure 2. Diel differences in CH_4 diffusion flux (**a**) and ebullition flux (**b**). (The black lines represent the median and white dots indicate the mean; lower and upper edges represent 25th and 75th, respectively; whiskers represent confidence intervals of 1.5 times the interquartile range; black dots indicate outliers).

4.2. Spatial Variation of CH_4 Ebullition Flux from Upstream to Downstream

Table 2 shows the dissolved CH_4 concentration, saturation, and contribution of CH_4 ebullition flux in the surface water of the Dahejia Reservoir in different subregion. As shown by Table 2, the CH_4 concentration in the surface water varied spatially within the range of 0.12–0.47 μmol L^{-1}. Specifically, in the River subregion, Middle subregion, Lake subregion, and Down subregion, the CH_4 concentration in the surface water fell within the ranges of 0.39–0.42 μmol L^{-1}, 0.18–0.28 μmol L^{-1}, 0.3–0.47 μmol L^{-1}, and 0.12–0.24 μmol L^{-1}, respectively. ANOVA revealed that the mean CH_4 concentration in the River subregion (0.4 ± 0.03 μmol L^{-1}) and the Lake subregion (0.39 ± 0.09 μmol L^{-1}) was significantly higher than that of the Middle subregion (0.23 ± 0.05 μmol L^{-1}) and the Down subregion (0.19 ± 0.06 μmol L^{-1}) ($p < 0.05$). The CH_4 saturation varied spatially within the range of 2297–8951%. In the River, Middle, Lake, and Down subregions, the CH_4 saturation fell within the ranges of 6645–7246%, 3314–4730%, 5904–8951%, and 2297–4617%, respectively. ANOVA revealed that the mean CH_4 saturation in the River subregion (6695 ± 779%) and the Lake subregion (7720 ± 1565%) was significantly higher than that of the Middle subregion (3310 ± 808%) and Down subregion (3514 ± 1164%) ($p < 0.05$). The dissolved CH_4 concentrations in the surface water of all subregions of the Dahejia Reservoir were all significantly higher than the equilibrium concentration of CH_4 in the atmosphere. The contribution of CH_4 ebullition flux in the River subregion to total CH_4 flux at the reservoir varied within the range of 52.98–88.7%; for the Middle, Lake, and Down subregions, it varied within the range of 96.3–99.43%, 43.69–79.05%, and 63.67–94.61%, respectively. Thus, the Dahejia Reservoir was an emission source of CH_4.

Table 2. Dissolved CH_4 concentration, saturation, and contribution of CH_4 ebullition flux in the Dahejia Reservoir in different subregion.

Subregion	CH_4 Concentration (μmol L^{-1})	CH_4 Saturation (%)	Contribution of CH_4 Ebullition Flux (%)
River	0.40 ± 0.03 ^{a}	6695 ± 779 ^{a}	70.84 ± 25.25 ^{a}
Middle	0.23 ± 0.05 ^{b}	3310 ± 808 ^{b}	98.27 ± 1.73 ^{b}
Lake	0.39 ± 0.09 ^{a}	7720 ± 1565 ^{a}	61.58 ± 17.69 ^{a}
Down	0.19 ± 0.06 ^{b}	3514 ± 1164 ^{b}	75.39 ± 16.78 ^{a}

^{a,b} Values having different subscript letters in the same column are significantly different from each other ($p < 0.05$).

Figure 3 shows the spatial characteristics of CH_4 diffusion flux and ebullition flux across the water—atmosphere interface in different subregions of the Dahejia Reservoir. The CH_4 diffusion flux across the water—atmosphere interface in the Dahejia Reservoir varied within the range of 0–0.21 mg m^{-2} h^{-1}. Specifically, the CH_4 diffusion flux in the River, Middle, Lake, and Down subregions varied within the range of 0.11–0.12 mg m^{-2} h^{-1}, 0–0.01 mg m^{-2} h^{-1}, 0.04–0.13 mg m^{-2} h^{-1}, and 0.04–0.21 mg m^{-2} h^{-1}, respectively. ANOVA showed that the mean CH_4 diffusion flux in the Down subregion (0.11 ± 0.09 mg m^{-2} h^{-1}) was significantly higher than that of the Middle subregion (0.01 ± 0.01 mg m^{-2} h^{-1}) ($p < 0.05$). However, the mean CH_4 diffusion flux of the Lake subregion (0.07 ± 0.05 mg m^{-2} h^{-1}) was not significantly different from that in the River subregion (0.11 ± 0.01 mg m^{-2} h^{-1}) ($p > 0.05$). As shown above, the mean CH_4 diffusion flux was higher in the upstream and downstream of the reservoir. The CH_4 ebullition flux varied within the range of 0.08–1.12 mg m^{-2} h^{-1}. Specifically, the CH_4 ebullition flux in the River, Middle, Lake, and Down subregions varied within the range of 0.12–0.92 mg m^{-2} h^{-1}, 0.08–1.12 mg m^{-2} h^{-1}, 0.08–0.15 mg m^{-2} h^{-1}, and 0.17–0.76 mg m^{-2} h^{-1}, respectively. ANOVA showed that the mean CH_4 ebullition flux in the River subregion (0.52 ± 0.57 mg m^{-2} h^{-1}), Middle subregion (0.51 ± 0.54 mg m^{-2} h^{-1}), Lake subregion (0.11 ± 0.04 mg m^{-2} h^{-1}), and Down subregion (0.43 ± 0.3 mg m^{-2} h^{-1}) were not significantly different ($p > 0.05$). From upstream to downstream, the mean CH_4 ebullition flux first decreased and then increased, with the minimum found in the Lake subregion. Taken together, ebullition was the primary mode of CH_4 emission in the Dahejia Reservoir.

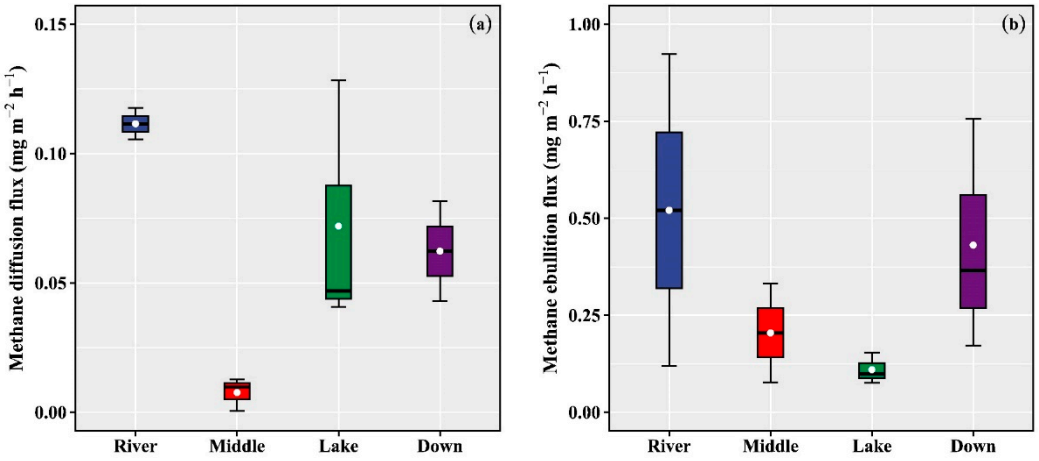

Figure 3. CH_4 diffusion flux (**a**) and ebullition flux (**b**) in different subregions (Symbols are similar to Figure 2).

5. Discussion

5.1. Influence of Abiotic Factors on CH_4 Ebullition Flux

We carried out the Spearman's rank correlation test for all data (Figure 4). The results showed that CH_4 ebullition flux was significantly positively correlated with total CH_4 flux (R = 0.94, $p < 0.05$). This finding demonstrated the considerable contribution made by CH_4 ebullition flux to total CH_4 flux. In other words, ebullition was a primary mode of CH_4 emissions from the reservoir. In the present study, we found that CH_4 ebullition flux was significantly negatively correlated with total organic carbon in the water (R = −0.66, $p < 0.05$) and total phosphorus in the sediment (R = −0.72, $p < 0.05$). Total organic carbon and total phosphorus have been identified as two limiting factors for primary productivity of the ecosystem [29,30]. The changes in ecosystem productivity may promote carbon dioxide generation and inhibit methane production in the Dahejia Reservoir. CH_4 ebullition flux was significantly positively correlated with sediment pH (R = 0.79, $p < 0.05$). It has been reported that pH variation resulted in changes in carbon source and sink of the aquatic ecosystem [31]. The higher the pH, the smaller the carbon dioxide emissions will be, which reduces the environmental pH. Within the suitable range of pH for methanogens,

the lower the pH, the higher the activity of the methanogens and the greater the amount of CH_4 produced [32]. CH_4 ebullition flux was significantly negatively correlated with nitrate in sediment ($R = -0.76$, $p < 0.05$). Relevant studies have shown that nitrate nitrogen promoted nitrous oxide generation and emissions, but had a negative correlation with CH_4 emissions [33]. Nitrous oxide is involved in CH_4 oxidation as electron receptors and can be used for methane oxidation coupled to denitrification. [34,35]. Therefore, an excessively high level of nitrate nitrogen inhibits CH_4 production. We found no significant correlation between the other environmental variables and CH_4 ebullition flux. This was possibly because we only studied the warm season.

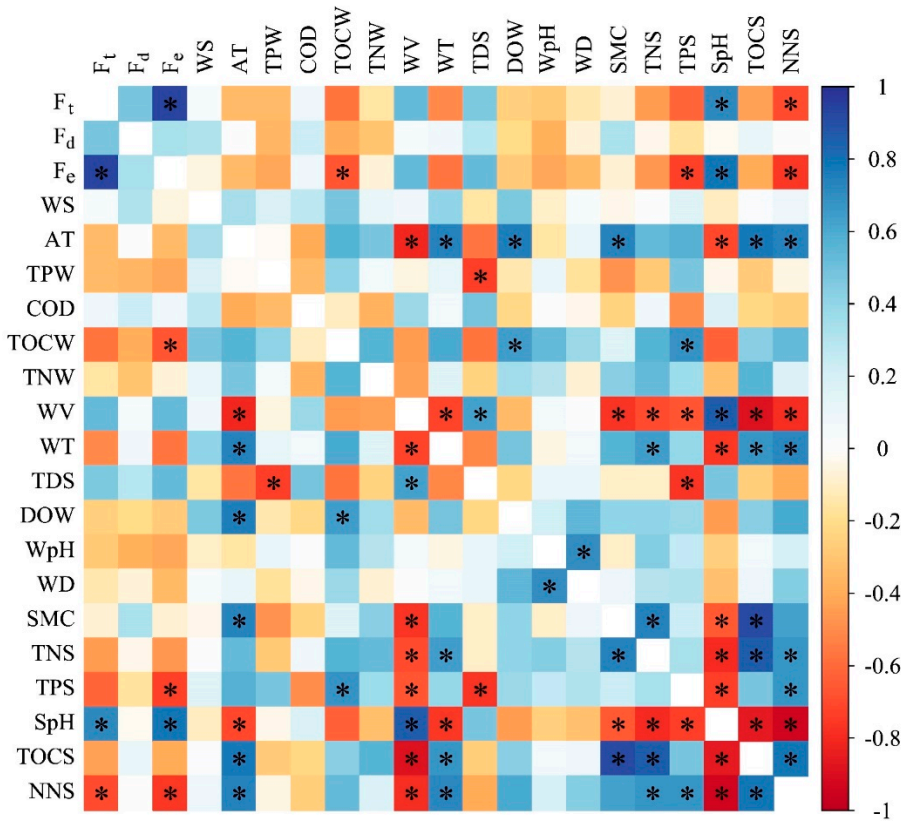

Figure 4. The correlations between CH_4 fluxes and physicochemical variables. Spearman's rank correlation coefficients are presented in the boxes in different colors. Blue represents positive correlation, red indicates negative correlation, and white means no correlation. The asterisks (*) mean the correlations are statistically significant ($p < 0.05$). (Abbreviation: F_t, total CH_4 flux; F_d, CH_4 diffusion flux; F_e, CH_4 ebullition flux; WS, wind speed; AT, Air temperature; TPW, total phosphorus in water; COD, chemical oxygen demand; TOCW, total organic carbon in water; TNW, total nitrogen in water; WV, water velocity; WT, water temperature; TDS, total dissolved solid; DOW, dissolved oxygen in water; WpH, water pH; WD, water depth; SMC, sediment moisture content; TNS, total nitrogen in sediment; TPS, total phosphorus in sediment; SpH, sediment pH; TOCS, total organic carbon in sediment; NNS, nitrate nitrogen in sediment).

5.2. Sediment Microbes Affected the CH_4 Ebullition Flux

CH_4 emissions from reservoirs implicate complex interactions between various factors, among which physicochemical variables only account for a certain proportion of CH_4 ebullition. CH_4 production and emissions from inland waters are largely associated with microbial activities [36]. To clarify the influence of microbial community composition and structure in sediments on CH_4 ebullition flux, we first performed a regression analysis between total microbial abundance in sediments and CH_4 ebullition flux. The results of the

analysis are shown in Figure 5. CH_4 ebullition flux had a significantly negative correlation with the total microbial abundance in sediments ($R^2 = 0.499$, $p = 0.009$).

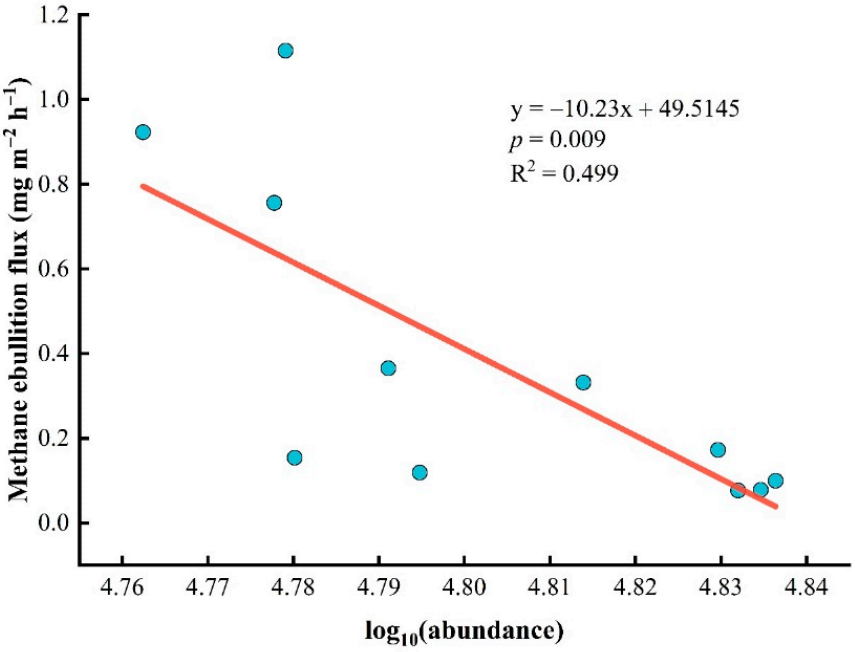

Figure 5. Regression analysis of CH_4 ebullition flux and the logarithm of microbial community abundance in sediments. The red line represents the fit of a linear regression through the observed data.

We further analyzed the influence of the abundance of different species on CH_4 ebullition flux. The microbial communities in sediments in different subregions were subjected to detrended correspondence analysis (DCA). The gradient lengths along the four axes were 0.1564, 0.0092, 0.0024, and 0, respectively, all of which were below 3. Therefore, we conducted a redundancy analysis (RDA) for the data. The results are shown in Figure 6. The explanation degrees of RDA1 and RDA2 for CH_4 ebullition flux were 96.68% and 0.56%, respectively. The two collectively explained 97.24% of CH_4 ebullition flux. Firmicutes and Verrucomicrobia were the main bacteria contributing to structural differentiation of microbial communities in sediments at the sampling points 1 and 3. Acidobacteria, Gemmatimonadetes, Epsilonbacteraeota, Chloroflexi, and Nitrospirae were the main bacteria contributing to structural differentiation of microbial communities in sediments at the sampling points 7, 8, and 9. Actinobacteria was the main contributor to structural differentiation of microbial communities in sediments at the sampling point 6. Bacteroidetes and Proteobacteria were the main contributors to structural differentiation of microbial communities in sediments at the sampling points 4 and 5 in the Middle subregion and at the sampling points 10, 11 and 12 in the Down subregion.

Total CH_4 flux and ebullition flux were positively correlated with the abundance of Firmicutes, Actinobacteria, and Verrucomicrobia, and negatively with Proteobacteria, Chloroflexi, Gemmatimonadetes, and Nitrospirae. The dissolved CH_4 concentration and CH_4 diffusion flux were positively correlated with the abundance of Firmicutes and Verrucomicrobia, and negatively with that of Bacteroidetes and Proteobacteria. Proteobacteria, Actinobacteria, Bacteroidetes, Gemmatimonadetes, and Nitrospirae actively participate in organic matter decomposition. These bacteria play crucial roles in the Earth's biochemical cycle of carbon, or even in sulfur cycle [37–39]. As shown in Figure 6, CH_4 ebullition flux and diffusion flux were negatively correlated with the abundance of Nitrospirae. Most species belonging to the Nitrospirae are nitrifying bacteria and are widely present in freshwater ecosystems. These bacteria can convert nitrites into nitrates and

compete with methanogens for substrates [40]. It has been reported that nitrous oxide and CH_4 emissions are negatively correlated with each other [33]. Due to the joint action of methanotrophs (typically *Methylocaldum* species) and denitrifying bacteria (typically *Thauera* species), nitrous oxide reduced CH_4 production while accelerating its oxidation. Besides, as the temperature rose, there would be a transition from the predominance of reduction of nitrous oxide to CH_4 oxidation [41]. Furthermore, the CH_4 ebullition flux and diffusion flux were also negatively correlated with the abundance of Proteobacteria. This is because Proteobacteria competes with methanogens for substrates, which promotes carbon dioxide and nitrous oxide emissions simultaneously. A large number of studies have shown that the relative abundance of Proteobacteria had a significantly positive correlation with carbon dioxide and nitrous oxide emissions [35,42]. The higher the abundance of Proteobacteria and Bacteroidetes in soil, the higher the carbon dioxide emissions would be [43]. It has been found that as primary producers, Epsilonbacteraeota is not only backbones of the ecosystem, but also participates extensively in the carbon and nitrogen cycles [44]. These bacteria use hydrogen or reductive sulfides as energy sources and produce nitrogen via the denitrification pathway, where nitrates act as electron receptors. Besides, Epsilonbacteraeota fixes carbon dioxide via the reductive tricarboxylic acid cycle (rTCA) to achieve autotrophic growth [45]. As analyzed above, composition changes of microbial communities in sediments are important biotic factors influencing CH_4 ebullition flux.

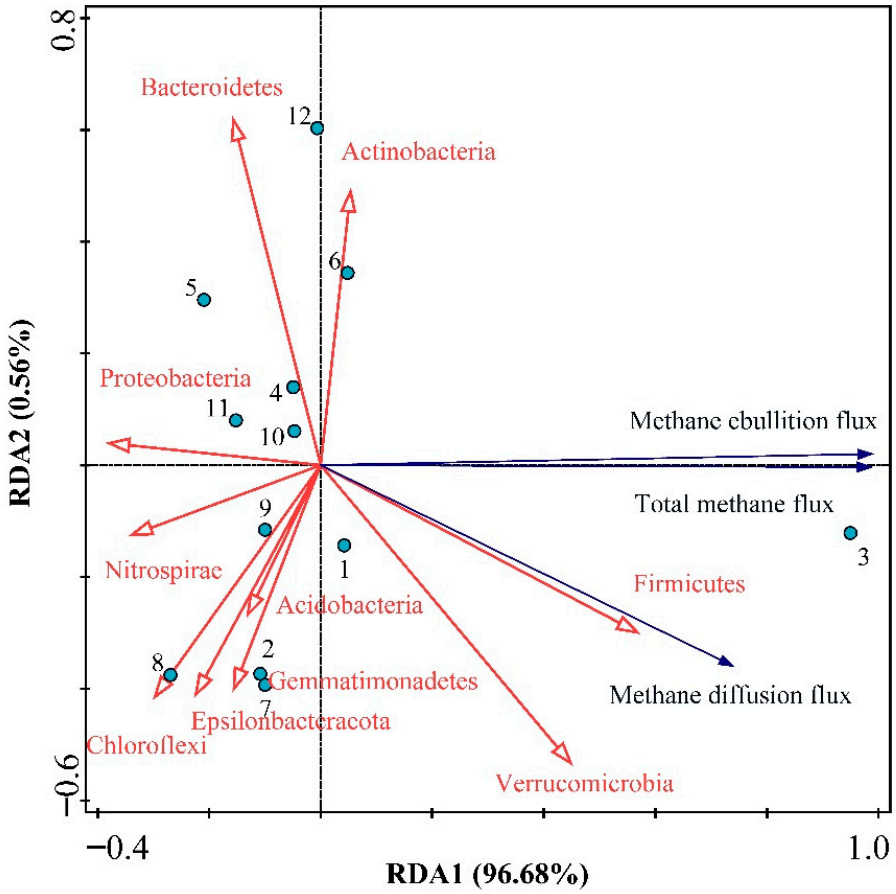

Figure 6. Redundancy analysis of the correlation between CH_4 fluxes and abundance of sediment microbes. Red arrows represent sediment microbial communities, black arrows indicate CH_4 fluxes, and blue dots represent sampling points (1–12).

5.3. Comparison of CH_4 Ebullition Flux at Reservoirs in Different Climate Zones

Table 3 shows the results of in-situ monitoring of CH_4 ebullition flux at several reservoirs in tropical, subtropical, and frigid zones. The CH_4 ebullition fluxes at reservoirs

in frigid zones are generally lower than those in tropical and subtropical zones. This is because the lower the latitude and the higher the temperature, the higher the microbial activity and the faster the CH_4 production will be [46]. The CH_4 ebullition flux varies significantly across the reservoirs, especially for tropical and subtropical reservoirs. The reasons for the variability include reservoir age, drainage subregion, land use pattern, eutrophication, and primary productivity [47,48]. Recent studies have shown extensive CH_4 ebullition flux in cold region of the north, a phenomenon that tends to be ignored and has been rarely discussed [49]. CH_4 is very likely to accumulate in reservoirs located in cold regions. An explosive growth of CH_4 flux is common in melt season [50]. As global warming gets worse, the melting of permafrost rich in organic matter leads to an increase in CH_4 emissions from the local water bodies [17]. For reservoirs in frigid zones, the maximum CH_4 ebullition flux can reach up to 115.59 mg m^{-2} h^{-1}. Dahejia Reservoir is also located in the subtropical zone, like Samuel Reservoir in Brazil and Pengxi River/Reservoir in the Three Gorges Reservoir Area, China. The CH_4 ebullition flux is of the same order of magnitude at the three reservoirs. However, the Dahejia Reservoir is located in the Qinghai-Tibet Plateau, where the climate more resembles that in the frigid zone. Therefore, the CH_4 ebullition flux in the Dahejia Reservoir is closer to that in Porttipahta Reservoir in Finland (0.4 mg m^{-2} h^{-1}) and Miaowei Reservoir in tropical China (0.33 $\pm$ 0.56 mg m^{-2} h^{-1}). Compared with the existing reports at home and abroad, the CH_4 ebullition flux across the water—atmosphere interface in the Dahejia Reservoir is at a moderate level. The contribution made by CH_4 ebullition flux to total CH_4 flux is comparable to that at other reservoirs at home and abroad.

As for the temporal and spatial characteristics on the reservoir scale, Grinham et al. observed a significant difference in CH_4 ebullition flux in the daytime and nighttime [51]. However, we did not observe a similar pattern of variation for the Dahejia Reservoir. From the upstream to the downstream of the reservoir, Yang et al. found that ebullition was the dominant mode of CH_4 emissions in the upstream of the Xin'anjiang Reservoir, while diffusion was dominant in the downstream [52]. Mcclure et al. showed that the CH_4 ebullition flux decreased from the upstream to the downstream of the Falling Creek Reservoir [53]. We observed a similar variation for the Dahejia Reservoir, except that the CH_4 ebullition flux in the Down subregion was significantly increased. Bai et al. reported similar findings for the Three Gorges Reservoir during the low water period. That is, the CH_4 ebullition flux was higher in the downstream (167.173 mg m^{-2} h^{-1}) than in the upstream (12.23–123.05 mg m^{-2} h^{-1}) [54]. As analyzed above, CH_4 ebullition flux has displayed significant temporal and spatial heterogeneity, either on the global or the reservoir scale. In the context of global climate change, the temperature rise in the Qinghai-Tibet Plateau is twice as much as the global average during the same period [55]. Moreover, the precipitation and air temperature vary consistently in the plateau region. Both have been increasing over the years. The increase in precipitation will accelerate organic matter decomposition, while that in air temperature can lead to eutrophication. They work synergistically to promote the geochemical cycling of carbon in water bodies [56]. The uniqueness of the plateau environment plus the action of several other factors has aggravated the spatial and temporal heterogeneity in CH_4 ebullition. However, our study was geographically confined to the Dahejia Reservoir, and the findings may not be applicable to CH_4 ebullition from reservoirs over the entire Qinghai-Tibet Plateau. It is necessary to choose more representative reservoirs in the Qinghai-Tibet Plateau to clarify the spatial and temporal features of CH_4 ebullition and the associated influence factors.

Table 3. CH_4 ebullition flux from global reservoirs.

Reservoir	CH_4 Ebullition Flux (mg m^{-2} h^{-1})	Contribution of CH_4 Ebullition Flux (%)	Note
Thirparappu [57]	114.47	95.07	Tropical
Miaowei [58]	0.33 ± 0.56	62.26	Tropical
Gatun Lake [59]	525.56	97.7	Tropical
Falling Greek [53]	0.67 ± 0.31	72.17	Subtropical
Xin'anjiang [52]	2.73 ± 2.02	92.86	Subtropical
Itaipu [60]	0.025	7	Subtropical
Samuel [60]	0.57	55.88	Subtropical
Pengxi River [7]	0.84	70	Subtropical
Saar River [61]	5.31 ± 7.46	97	Temperate zone
Eguzon [62]	0.24 ± 0.56	9.8	Temperate zone
Northern Québec [63]	0.1	83	Frigid zone
Porttipahta [6]	0.4	17.09	Frigid zone
Lokka [63]	115.59	83.63	Frigid zone
Dahejia	0.31 ± 0.29	86.11	This study

6. Conclusions

It should be noted that since global warming has been deteriorating, the uncertainty of CH_4 ebullition from reservoirs located in the Qinghai-Tibet Plateau will increase considerably [17,19]. We studied CH_4 ebullition flux from the Dahejia Reservoir located in the upper reaches of the Yellow River and analyzed the spatial and temporal characteristics of CH_4 ebullition flux, the contribution made by CH_4 ebullition flux to total CH_4 flux, and the influence factors during the warm season (from July–August 2021). We arrived at the following conclusions:

1. CH_4 ebullition was the dominant mode of CH_4 emissions at the study site and contributed to 78.85 ± 20% of total CH_4 flux.
2. The CH_4 ebullition flux in the nighttime (0.34 ± 0.21 mg m^{-2} h^{-1}) was significantly higher than that in the daytime (0.19 ± 0.21 mg m^{-2} h^{-1}).
3. The CH_4 ebullition flux first decreased and then increased from upstream to downstream. In the River, Middle, Lake, and Down subregions, the CH_4 ebullition flux was 0.52 ± 0.57 mg m^{-2} h^{-1}, 0.51 ± 0.54 mg m^{-2} h^{-1}, 0.11 ± 0.04 mg m^{-2} h^{-1}, and 0.43 ± 0.3 mg m^{-2} h^{-1}, respectively.
4. Among abiotic variables, the CH_4 ebullition flux was closely related to total phosphorus, total organic carbon, pH and nitrate nitrogen. Among biotic factors, CH_4 ebullition flux had a significant negative linear correlation with microbial abundance. The redundancy analysis showed that the CH_4 ebullition flux was significantly positively correlated with the abundances of Firmicutes and Actinobacteria and negatively with that of Proteobacteria and Chloroflexi.

Although we had studied the CH_4 ebullition flux of the Dahejia Reservoir on the diel scale, our study still had the following limitations due to limited time and manpower. We had discussed the diel and spatial variations of CH_4 ebullition flux across the water-atmosphere interface in the Dahejia Reservoir of the Yellow River. In the future, we need to further investigate the monthly, seasonal, and interannual variations of CH_4 ebullition flux in the study site, especially the variations in the cold season. Specifically, we will include all microbes in the water bodies of the reservoir into our study. Microbial genome data will be collected in a more comprehensive manner by metagenomic high-throughput sequencing, so as to precisely quantify CH_4 ebullition.

Author Contributions: Methodology, W.T., F.X. and H.J.; data curation, X.M. and L.X.; writing—review and editing, Y.W., Y.Y. and H.Y. All authors have read and agreed to the published version of the manuscript.

Funding: The research work was supported by the National Natural Science Foundation of China (Project No. 52070108), the Basic Research Program of Qinghai Province (2022-ZJ-718) and the Qinghai Province innovation platform construction project (2020-ZJ-Y06).

Institutional Review Board Statement: Not applicable.

Informed Consent Statement: Not applicable.

Data Availability Statement: The data presented in this study are available in the article.

Acknowledgments: We thank reviewers for their constructive comments and suggestions to improve the early version of this paper.

Conflicts of Interest: The authors declare no conflict of interest.

References

1. WMO. The State of Greenhouse Gases in the Atmosphere Based on Global Observations through 2020. *WMO Greenh. Gas Bull.* **2021**, *17*, 1–3.
2. IPCC. Climate Change 2013: The Physical Science Basis. In *Contribution of Working Group I to the Fifth Assessment Report of the Intergovernmental Panel on Climate Change*; Stocker, T.F., Qin, D., Plattner, G.-K., Tignor, M., Allen, S., Boschung, J., Nauels, A., Xia, Y., Bex, V., Midgley, P., Eds.; Cambridge University Press: Cambridge, UK; New York, NY, USA, 2013; p. 1535.
3. Agasild, H.; Zingel, P.; Tuvikene, L.; Tuvikene, A.; Timm, H.; Feldmann, T.; Salujõe, J.; Toming, K.; Jones, R.; Nõges, T. Biogenic methane contributes to the food web of a large, shallow lake. *Freshw. Biol.* **2014**, *59*, 272–285. [CrossRef]
4. Dlugokencky, E.J. Trends in Atmospheric Methane (NOAA/GML, 2021). Available online: https://www.esrl.noaa.gov/gmd/ccgg/trends_ch4 (accessed on 18 September 2021).
5. Zhang, P.; Wang, X.F.; Yuan, X.Z. General characteristics and research progress of methane emissions from freshwater ecosystems in China. *China Environ. Sci.* **2020**, *40*, 3567–3579. [CrossRef]
6. Bastviken, D.; Tranvik, L.J.; Downing, J.A.; Crill, P.M.; Enrich-Prast, A. Freshwater Methane Emissions Offset the Continental Carbon Sink. *Science* **2011**, *331*, 50. [CrossRef]
7. Li, Z.; Zhang, C.; Liu, L. Ebullition fluxes of CO_2 and CH_4 in Pengxi River, Three Gorges Reservoir. *J. Lake Sci.* **2014**, *26*, 789–798.
8. Linkhorst, A.; Paranaíba, J.R.; Mendonça, R.; Rudberg, D.; DelSontro, T.; Barros, N.; Sobek, S. Spatially Resolved Measurements in Tropical Reservoirs Reveal Elevated Methane Ebullition at River Inflows and at High Productivity. *Glob. Biogeochem. Cycles* **2021**, *35*, e2020GB006717. [CrossRef]
9. DelSontro, T.; Boutet, L.; St-Pierre, A.; del Giorgio, P.A.; Prairie, Y.T. Methane ebullition and diffusion from northern ponds and lakes regulated by the interaction between temperature and system productivity. *Limnol. Oceanogr.* **2016**, *61*, S62–S77. [CrossRef]
10. West, W.E.; Creamer, K.P.; Jones, S.E. Productivity and depth regulate lake contributions to atmospheric methane. *Limnol. Oceanogr.* **2016**, *61*, S51–S61. [CrossRef]
11. Saunois, M.; Stavert, A.R.; Poulter, B.; Bousquet, P.; Canadell, J.G.; Jackson, R.B.; Raymond, P.A.; Dlugokencky, E.J.; Houweling, S.; Patra, P.K.; et al. The Global Methane Budget 2000-2017. *Earth Syst. Sci. Data* **2020**, *12*, 1561–1623. [CrossRef]
12. Houghton, K.M.; Carere, C.R.; Stott, M.B.; McDonald, I.R. Thermophilic methanotrophs: In hot pursuit. *Fems Microbiol. Ecol.* **2019**, *95*, fiz125. [CrossRef]
13. Ding, J.; Lu, Y.-Z.; Fu, L.; Ding, Z.-W.; Mu, Y.; Cheng, S.H.; Zeng, R.J. Decoupling of DAMO archaea from DAMO bacteria in a methane-driven microbial fuel cell. *Water Res.* **2017**, *110*, 112–119. [CrossRef] [PubMed]
14. Chowdhury, T.R.; Dick, R.P. Ecology of aerobic methanotrophs in controlling methane fluxes from wetlands. *Appl. Soil Ecol.* **2013**, *65*, 8–22. [CrossRef]
15. Ren, M.F.; Li, L.Y.; Chen, L.; Xing, T.T.; Liu, Y.Q.; Dong, X.Z. Methanogen communities and predominant methanogenic pathways in three saline-alkaline lakes on the Tibetan Plateau. *Acta Microbiol. Sin.* **2020**, *60*, 161–171. [CrossRef]
16. Ma, X.F.; Chen, S.Y.; Deng, J.; Feng, Q.S.; Huang, X.D. Vegetation phenology dynamics and its response to climate change on the Tibetan Plateau. *Acta Prataculturae Sin.* **2016**, *25*, 13–21. [CrossRef]
17. Zhang, L.; Xia, X.; Liu, S.; Zhang, S.; Li, S.; Wang, J.; Wang, G.; Gao, H.; Zhang, Z.; Wang, Q.; et al. Significant methane ebullition from alpine permafrost rivers on the East Qinghai-Tibet Plateau. *Nat. Geosci.* **2020**, *13*, 349–354. [CrossRef]
18. Natchimuthu, S.; Sundgren, I.; Gålfalk, M.; Klemedtsson, L.; Crill, P.; Danielsson, Å.; Bastviken, D. Spatio-temporal variability of lake CH_4 fluxes and its influence on annual whole lake emission estimates. *Limnol. Oceanogr.* **2016**, *61*, S13–S26. [CrossRef]
19. Wang, L.; Du, Z.; Wei, Z.; Xu, Q.; Feng, Y.; Lin, P.; Lin, J.; Chen, S.; Qiao, Y.; Shi, J.; et al. High methane emissions from thermokarst lakes on the Tibetan Plateau are largely attributed to ebullition fluxes. *Sci. Total Environ.* **2021**, *801*, 149692. [CrossRef]
20. Harrison, J.A.; Deemer, B.R.; Birchfield, M.K.; O'Malley, M.T. Reservoir Water-Level Drawdowns Accelerate and Amplify Methane Emission. *Environ. Sci. Technol.* **2017**, *51*, 1267–1277. [CrossRef]
21. DelSontro, T.; Perez, K.K.; Sollberger, S.; Wehrli, B. Methane dynamics downstream of a temperate run-of-the-river reservoir. *Limnol. Oceanogr.* **2016**, *61*, S188–S203. [CrossRef]
22. Conrad, R.; Ji, Y.; Noll, M.; Klose, M.; Claus, P.; Enrich-Prast, A. Response of the methanogenic microbial communities in Amazonian oxbow lake sediments to desiccation stress. *Environ. Microbiol.* **2014**, *16*, 1682–1694. [CrossRef]

23. Zhu, D.; Wu, Y.; Chen, H.; He, Y.; Wu, N. Intense methane ebullition from open water area of a shallow peatland lake on the eastern Tibetan Plateau. *Sci. Total Environ.* **2016**, *542*, 57–64. [CrossRef] [PubMed]
24. Li, Q.Q. Aquatic Ecological Environmental Impact Assessment of Dahejia Hydropower Station Project. Master's Thesis, Xi'an University of Technology, Xi'an, China, 2017.
25. Johnson, K.M.; Hughes, J.E.; Donaghay, P.L.; Sieburth, J.M. Bottle-calibration static head space method for the determination of methane dissolved in seawater. *Anal. Chem.* **1990**, *62*, 2408–2412. [CrossRef]
26. Wanninkhof, R. Relationship between wind speed and gas exchange over the ocean revisited. *Limnol. Oceanogr. Methods* **2014**, *12*, 351–362. [CrossRef]
27. Modi, A.; Vai, S.; Caramelli, D.; Lari, M. The Illumina Sequencing Protocol and the NovaSeq 6000 System. *Methods Mol. Biol.* **2021**, *2242*, 15–42. [CrossRef]
28. Edgar, R.C. Search and clustering orders of magnitude faster than BLAST. *Bioinformatics* **2010**, *26*, 2460–2461. [CrossRef] [PubMed]
29. Beaulieu, J.J.; DelSontro, T.; Downing, J.A. Eutrophication will increase methane emissions from lakes and impoundments during the 21st century. *Nat. Commun.* **2019**, *10*, 1375. [CrossRef]
30. Xiao, Q.; Zhang, M.; Hu, Z.; Gao, Y.; Hu, C.; Liu, C.; Liu, S.; Zhang, Z.; Zhao, J.; Xiao, W.; et al. Spatial variations of methane emission in a large shallow eutrophic lake in subtropical climate. *J. Geophys. Res. Biogeosciences* **2017**, *122*, 1597–1614. [CrossRef]
31. He, B.; He, J.; Wang, J.; Li, J.; Wang, F. Characteristics of GHG flux from water-air interface along a reclaimed water intake area of the Chaobai River in Shunyi, Beijing. *Atmos. Environ.* **2018**, *172*, 102–108. [CrossRef]
32. Garcia, J.-L.; Patel, B.K.C.; Ollivier, B. Taxonomic, Phylogenetic, and Ecological Diversity of Methanogenic Archaea. *Anaerobe* **2000**, *6*, 205–226. [CrossRef]
33. Smith, R.L.; Bohlke, J.K. Methane and nitrous oxide temporal and spatial variability in two midwestern USA streams containing high nitrate concentrations. *Sci. Total Environ.* **2019**, *685*, 574–588. [CrossRef]
34. Ettwig, K.F.; Butler, M.K.; Le Paslier, D.; Pelletier, E.; Mangenot, S.; Kuypers, M.M.; Schreiber, F.; Dutilh, B.E.; Zedelius, J.; de Beer, D.; et al. Nitrite-driven anaerobic methane oxidation by oxygenic bacteria. *Nature* **2010**, *464*, 543–548. [CrossRef] [PubMed]
35. Yang, B. N_2O and CH_4 Fluxes and Their Influencing Factors in Spartina Alterniflora Salt Marsh in Nanhui Shore of Yangtze Estuary under High Nitrogen Background. Ph.D. Thesis, East China Normal University, Shanghai, China, 2021.
36. Yvon-Durocher, G.; Allen, A.P.; Bastviken, D.; Conrad, R.; Gudasz, C.; St-Pierre, A.; Thanh-Duc, N.; Del Giorgio, P.A. Methane fluxes show consistent temperature dependence across microbial to ecosystem scales. *Nature* **2014**, *507*, 488–491. [CrossRef] [PubMed]
37. Ma, S.; Fang, C.; Sun, X.; Han, L.; He, X.; Huang, G. Bacterial community succession during pig manure and wheat straw aerobic composting covered with a semi-permeable membrane under slight positive pressure. *Bioresour. Technol.* **2018**, *259*, 221–227. [CrossRef] [PubMed]
38. Emerson, J.B.; Varner, R.K.; Wik, M.; Parks, D.H.; Neumann, R.B.; Johnson, J.E.; Singleton, C.M.; Woodcroft, B.J.; Tollerson, R.; Owusu-Dommey, A.; et al. Diverse sediment microbiota shape methane emission temperature sensitivity in Arctic lakes. *Nat. Commun.* **2021**, *12*, 5815. [CrossRef]
39. Bolhuis, H.; Cretoiu, M.S.; Stal, L.J. Molecular ecology of microbial mats. *Fems Microbiol. Ecol.* **2014**, *90*, 335–350. [CrossRef]
40. Kuypers, M.M.M.; Marchant, H.K.; Kartal, B. The microbial nitrogen-cycling network. *Nat. Rev. Microbiol.* **2018**, *16*, 263–276. [CrossRef]
41. Cheng, C. Research on Simultaneous Reduction and Mechanisms of Methane and Nitrous Oxide. Ph.D. Thesis, Shandong University, Jinan, China, 2019.
42. Li, J. Key Driving Factors Of Greenhouse Gas Fluxes Under Diffrent Microhabitats in Ulansuhai Wetland. Master's Thesis, Inner Mongolia University, Huhehaote, China, 2021.
43. Wei, H. Soil Greenhouse Gas Emission And Its Influencing Factors from Temperate Deciduous Broad-Leaved Forest And Tropical Mountain Rain Forest. Ph.D. Thesis, Northwest A & F University, Xianyang, China, 2018.
44. Hou, J.L. Metagenomic Study of the Structure, Evolution and Metabolic Potential of Microbial Communities Inhabiting Deep Sea Hydrothermal Chimneys. Master Thesis, Shanghai Jiao Tong University, Shanghai, China, 2018.
45. Campbell, B.J.; Engel, A.; Porter, M.L.; Takai, K. The versatile ε-proteobacteria: Key players in sulphidic habitats. *Nat. Rev. Microbiol.* **2006**, *4*, 458–468. [CrossRef]
46. Gao, Y.H. Study on CH_4 and N_2O Emission Characteristics and Influencing Factors of Reservoirs in Cold Regions. Master's Thesis, Dalian University of Technology, Dalian, China, 2019.
47. Isidorova, A.; Grasset, C.; Mendonça, R.; Sobek, S. Methane formation in tropical reservoirs predicted from sediment age and nitrogen. *Sci. Rep.* **2019**, *9*, 11017. [CrossRef]
48. Borges, A.V.; Darchambeau, F.; Teodoru, C.R.; Marwick, T.R.; Tamooh, F.; Geeraert, N.; Omengo, F.O.; Guérin, F.; Lambert, T.; Morana, C.; et al. Globally significant greenhouse-gas emissions from African inland waters. *Nat. Geosci.* **2015**, *8*, 637–642. [CrossRef]
49. Deemer, B.R.; Harrison, J.A.; Li, S.; Beaulieu, J.J.; DelSontro, T.; Barros, N.; Bezerra-Neto, J.F.; Powers, S.M.; dos Santos, M.A.; Vonk, J.A. Greenhouse Gas Emissions from Reservoir Water Surfaces: A New Global Synthesis. *BioScience* **2016**, *66*, 949–964. [CrossRef]

50. Neumann, R.B.; Moorberg, C.J.; Lundquist, J.D.; Turner, J.C.; Waldrop, M.P.; McFarland, J.W.; Euskirchen, E.S.; Edgar, C.W.; Turetsky, M.R. Warming Effects of Spring Rainfall Increase Methane Emissions From Thawing Permafrost. *Geophys. Res. Lett.* **2019**, *46*, 1393–1401. [CrossRef]
51. Grinham, A.; Dunbabin, M.; Albert, S. Importance of sediment organic matter to methane ebullition in a sub-tropical freshwater reservoir. *Sci. Total Environ.* **2018**, *621*, 1199–1207. [CrossRef] [PubMed]
52. Yang, L. Contrasting methane emissions from upstream and downstream rivers and their associated subtropical reservoir in eastern China. *Sci. Rep.* **2019**, *9*, 8072. [CrossRef]
53. McClure, R.P.; Lofton, M.E.; Chen, S.; Krueger, K.M.; Little, J.C.; Carey, C.C. The Magnitude and Drivers of Methane Ebullition and Diffusion Vary on a Longitudinal Gradient in a Small Freshwater Reservoir. *J. Geophys. Res. Biogeosciences* **2020**, *125*, 18. [CrossRef]
54. Bai, X.; Xu, Q.; Li, H.; Cheng, C.; He, Q. Lack of methane hotspot in the upstream dam: Case study in a tributary of the Three Gorges Reservoir, China. *Sci. Total Environ.* **2020**, *754*, 142151. [CrossRef]
55. Yao, T.; Dong. A comprehensive study of Water-Ecosystem-Human activities reveals unbalancing Asian Water Tower and accompanying potential risks. *Chin. Sci. Bull.* **2019**, *64*, 2761–2762. [CrossRef]
56. Sinha, E.; Michalak, A.M.; Balaji, V. Eutrophication will increase during the 21st century as a result of precipitation changes. *Science* **2017**, *357*, 405–408. [CrossRef] [PubMed]
57. Selvam, B.P.; Natchimuthu, S.; Arunachalam, L.; Bastviken, D. Methane and carbon dioxide emissions from inland waters in India–implications for large scale greenhouse gas balances. *Glob. Chang. Biol.* **2014**, *20*, 3397–3407. [CrossRef]
58. Liu, L.; Yang, Z.; Delwiche, K.; Long, L.; Liu, J.; Liu, D.; Wang, C.; Bodmer, P.; Lorke, A. Spatial and temporal variability of methane emissions from cascading reservoirs in the Upper Mekong River. *Water Res.* **2020**, *186*, 116319. [CrossRef]
59. Keller, M.; Stallard, R.F. Methane emission by bubbling from Gatun Lake, Panama. *J. Geophys. Res. Atmos.* **1994**, *99*, 8307–8319. [CrossRef]
60. dos Santos, M.A.; Rosa, L.P.; Sikar, B.; Sikar, E.; dos Santos, E.O. Gross greenhouse gas fluxes from hydro-power reservoir compared to thermo-power plants. *Energy Policy* **2006**, *34*, 481–488. [CrossRef]
61. Maeck, A.; DelSontro, T.; McGinnis, D.; Fischer, H.; Flury, S.; Schmidt, M.; Fietzek, P.; Lorke, A. Sediment Trapping by Dams Creates Methane Emission Hot Spots. *Environ. Sci. Technol.* **2013**, *47*, 8130–8137. [CrossRef] [PubMed]
62. Descloux, S.; Chanudet, V.; Serça, D.; Guérin, F. Methane and nitrous oxide annual emissions from an old eutrophic temperate reservoir. *Sci. Total Environ.* **2017**, *598*, 959–972. [CrossRef] [PubMed]
63. Huttunen, J.T.; Väisänen, T.S.; Hellsten, S.K.; Heikkinen, M.; Nykänen, H.; Jungner, H.; Niskanen, A.; Virtanen, M.O.; Lindqvist, O.V.; Nenonen, O.S.; et al. Fluxes of CH_4, CO_2, and N_2O in hydroelectric reservoirs Lokka and Porttipahta in the northern boreal zone in Finland. *Glob. Biogeochem. Cycles* **2002**, *16*, 3-1–3-17. [CrossRef]